01 Jan 2023

Application of a Variable Path Length Repetitive Process Control for Direct Energy Deposition of Thin-Walled Structures

Elias B. Snider

Douglas A. Bristow
Missouri University of Science and Technology, dbristow@mst.edu

Recommended Citation

E. B. Snider and D. A. Bristow, "Application of a Variable Path Length Repetitive Process Control for Direct Energy Deposition of Thin-Walled Structures," *2023 IEEE Conference on Control Technology and Applications, CCTA 2023*, pp. 150 - 155, Institute of Electrical and Electronics Engineers, Jan 2023.
The definitive version is available at https://doi.org/10.1109/CCTA54093.2023.10252574

2023 IEEE Conference on Control Technology and Applications (CCTA)
August 16-18, 2023. Bridgetown, Barbados

Application of a Variable Path Length Repetitive Process Control for Direct Energy Deposition of Thin-Walled Structures

Elias B. Snider and Douglas A. Bristow

2023 IEEE Conference on Control Technology and Applications (CCTA) | 979-8-3503-3544-6/23/$31.00 ©2023 IEEE | DOI: 10.1109/CCTA54093.2023.10252574

Abstract— **Direct Energy Deposition (DED) additive manufacturing is well suited to fabricating large thin-walled metal structures such as rocket nozzles but suffers from layer-to-layer defect propagation. Propagating defects may exhibit as slumping or a ripple in bead geometry. Recent works have used Repetitive Process Control (RPC) methods for additive manufacturing to stabilize the layer-wise defect propagation, but these methods require repetition of the same path. However, typical thin-wall DED applications, sometimes referred to as vase structures, have changing paths with each layer such as expanding or contracting diameters and changing profiles. This paper presents an extension to optimal RPC that uses a geometric mapping method in the learning algorithm to project previous layer defects onto the current layer, even when paths are of differing profile and length. The novel method is implemented on a DED system and sample parts with layer-changing geometry are printed. The experimental results demonstrate that the method is capable of stabilizing the layer-to-layer ripple instability and producing parts of good quality.**

I. Introduction

Metal additive manufacturing (AM) is a rich area of research. It is a relatively new manufacturing technology that has gained much traction in industry as a method of producing cost-effective prototypes with a short turn-around time as well as for small-quantity applications for parts which require very complex or difficult to machine geometry and material properties. Direct Energy Deposition (DED) processes utilizing a blown powder approach can further reduce costs compared to powder bed methods by reducing the amount of metal powder needed to manufacture these parts, while also increasing the flexibility of the machine for production of parts with varied sizes. One of the major difficulties in DED part production is the print quality of parts with respect to powder bed prints and traditional machining processes.

To minimize the effect of disturbances and propagation of errors in AM applications, many works have implemented layer-to-layer control. As pointed out by Altin, layer-to-layer control of AM systems is an attractive alternative to real-time control in terms of sensing requirements and computational simplicity [1] which is especially true for DED environments. Initial work in layer-to-layer correction concerned using iterative learning control (ILC), in which the process is assumed not to carry any previous errors into successive layers, in tangent with other control structures to reduce errors in the build height from a laser metal deposition machine [2, 3, 4].

More rigorous iterative controls formulations have been further developed to handle a variety of applications by applying spatial ILC in electrohydrodynamic jet printing [1], [5, 6, 7]. ILC has also been applied to selective laser melting (SLM) processes to demonstrate finite element simulated convergence of melt pool temperature errors [8, 9] and for temperature control of the melt pool in a SLM machine [10].

The ILC-based control structures, however, neglect any effect of previous layer errors on successive layer deposition. Repetitive process control (RPC) structures, in contrast, include layer-to-layer process dynamics are in the process modeling. The modeling of the blown powder DED manufacturing process as a repetitive process was formulated in [11, 12]. Simulations with general RPC [13] followed by a model predictive control approach in [14] demonstrated good performance and error convergence. Expanding on the modeling of the process, an RPC controller was developed and implemented on a DED manufacturing system to produce straight-wall builds with greatly improved part quality in [15, 16].

Using the same system, a quadratic optimal control approach was developed and implemented on much more complex build geometries in [17]. The specimens produced in these set of experiments utilized a five-axis DED machine and included a constant cross section with rotations of the build plate at each layer in their construction. The result was a non-constant reference in position which varied slowly from layer to layer. The implemented RPC very cleanly tracked the reference for the entirety of the build, resulting in extremely high-quality prints considering geometrical complexity [18].

All of these control structures, however, assume that the geometry of the build remains constant from layer to layer. The objective of this work was to widen the scope of a RPC structure for AM to include additive builds that contain changing geometry as the deposition progresses. The DED process control methods in [16, 19, 20, 21], serve as a foundation for the expansion of this framework to single-wall builds, with the objective of creating a control structure that is capable of stabilizing builds with variable path length resulting in overhangs. These structures present additional challenges to DED systems as overhangs tend to exacerbate rippling in wall builds and lead to poor final build quality.

The remainder of the paper is organized as follows. Background on RPC methods for layer-to-layer control of DED are summarized in Section II. Section III presents a

E.B. Snider and D.A. Bristow* are with the Department of Mechanical and Aerospace Engineering at the Missouri University of Science and Technology, Rolla, MO 65409 USA (*corresponding author e-mail: dbristow@mst.edu)

mapping method for propagating defect measurements from one layer to the next layer of differing path length. Section IV presents an optimal control formulation utilizing the layer-to-layer mapping. Experimental results are presented in Section V and concluding remarks are given in Section VI.

II. Repetitive Process Control of DED Processes

A. Build Geometry and Path Mapping

A simple cylinder is a good example of a typical thin-walled structure that may be produced by a DED process. The cylinder is constructed by successive circular depositions, incrementing in z at each layer as shown in Figure 1. The reference (as designated in the dashed lines at each layer) denotes the desired deposition height where the actual deposition height (in the z-direction) is represented in solid blue.

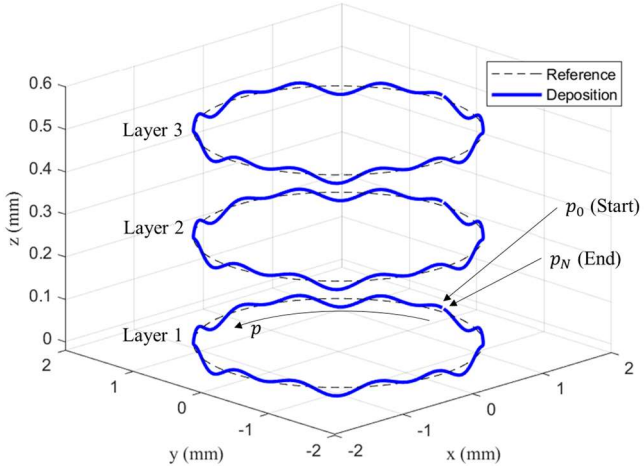

Figure 1: Typical Deposition Path of Cylinder Build

Plotting parameters as a function of the path length (as in Figure 2) allows for visualization of parameters such as layer height and error as a function of distance travelled from the beginning of that layer's deposition (p_0). For a uniform path at each layer, points along the path at a given layer will directly correspond to points on the paths of successive layers.

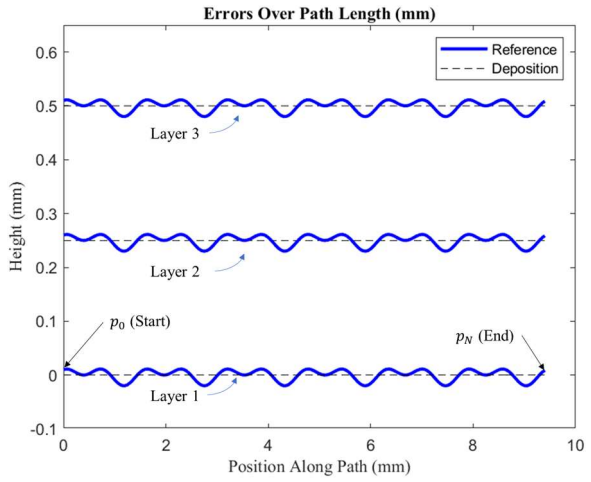

Figure 2: Errors Along the Layer Paths of a Cylinder Build

B. Process Modeling

For layer-to-layer error correction, the laser metal DED process is best described mathematically with a lifted-system representation of the process dynamics. Significant, in-depth modeling constructed in [20, 21] were expanded on to produce these results. The following provides a simplified summary of the mathematical structure serving as a basis for these expansions. The error at future layers is dependent on the control input,

$$e_{j+1} = Ae_j + Bu_{j+1}, \tag{1}$$

where,

$$e_{j+1} = \begin{bmatrix} e_{j+1}(0) & e_{j+1}(1) & \cdots & e_{j+1}(N-1) \end{bmatrix}^T, \tag{2}$$

$$u_{j+1} = \begin{bmatrix} u_{j+1}(0) & u_{j+1}(1) & \cdots & u_{j+1}(N-1) \end{bmatrix}^T, \tag{3}$$

are the stacked vectors of spatially sampled height error, $e_j(k)$, and deposition rate input, $u_j(k)$, respectively, at layer j and sample k along the path, and A and B contain the process dynamics. Process dynamics are constructed from linear convolution models as follows. Consider the non-causal impulse response of a linear process, $a(k)$ with support $k \in [-b, c]$, as illustrated in Figure 3. The process response from input $e_j(k)$ to output $e_{j+1}(k)$ can be solved with the convolution operation as,

$$e_{j+1}(k) = \sum_{i=-b}^{c} a(i) e_j(k-i). \tag{4}$$

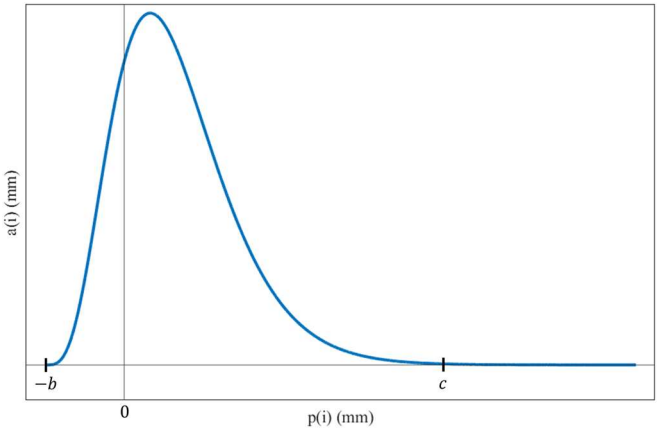

Figure 3: Non-Causal Impulse Response of Metal Deposition

For closed paths (paths in which the start and end points coincide such as circular toolpaths), the kernel function can be modified as,

$$a_{cp}(i) = \begin{cases} a(i) & ,0 \le i \le c \\ 0 & ,c < i < N-b \\ a(N-i) & ,N-b \le i < N \end{cases} \tag{5}$$

as illustrated in Figure 4. In the experimental implementation provided, a describes the impulse response of the error a the successive layer, e_{j+1}, to an error in the current layer, e_j.

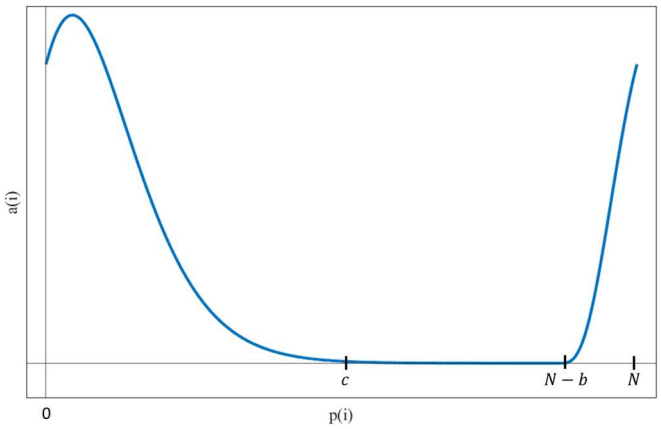

Figure 4: Closed-Path Impulse Response of Metal Deposition

The process dynamics matrix can then be solved as $A = \left[\alpha_{ij} \right]$, where,

$$\alpha_{ij} = \begin{cases} a_{cp}(i-j) & , i-j \geq 0 \\ a_{cp}(N-i+j) & , i-j < 0 \end{cases}. \quad (6)$$

The matrix B follows an identical construction to relate the input (a table feed velocity command in the case of the experimental implementation) to the error, using the impulse response of the input signal.

III. A Model for Variable Path Geometry and Path Length

While traditional RPC is a powerful and proven [16] method to overcome inherent instabilities in DED processes, the existing structures are restricted in the types of structures to which they may be applied; additive builds utilizing RPC methods as they have been presented thus far have layer-invariant tool paths and path lengths. While there are certainly applications for such cases, there are a many situations in which a varied toolpath is necessary for a part to be useful in its application.

A. Variable Build Geometry and Path Mapping

For the purposes of this paper, a cone geometry (a circular toolpath with increasing radius at successive layers) was chosen for exploring application of RPC to varied path lengths. Figure 5 depicts a set of simple, concentric toolpaths of increasing radius at each layer. Note that α defines the slope of the cone shape and determines the rate of increase in diameters at successive layers. A value of 50° is shown for α in Figure 5 and Figure 6 in order to emphasize the geometry and nuances of a changing path length, but a value of 10° was selected as a more conservative value in experimental trials presented later.

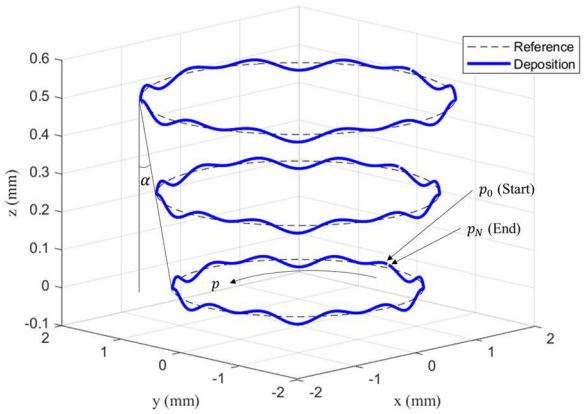

Figure 5: Deposition Path of a Cone Build

To adapt this framework to handle wall-builds which grow in length at successive layers (thus developing an overhang angle), an error vector large enough to contain the error values of the final layer (N_{max}) is first initialized with zeros. This approach allows the overall dimensions of the error vector as well as A and B matrices to remain constant throughout the build and at each layer. The error values from the current layer are filled, and the remaining space at the end of the error vector remains as a set of zeros.

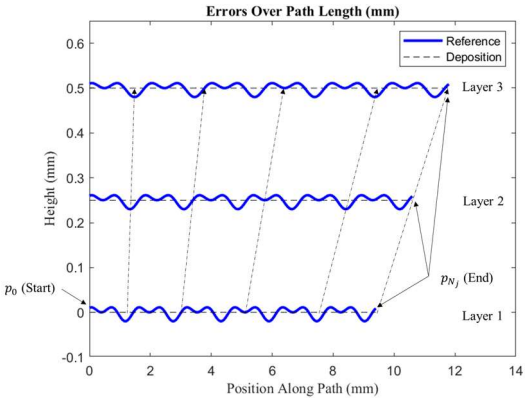

Figure 6: Errors Along the Layer Paths of a Cone Build

B. Modeling Adaptations

In order to handle the mismatched dimensions of A to the number of error points for a given layer (i.e. that the Toeplitz structure A is constructed in order to accommodate the longest path length), the cyclic portions of A must be recast such that the they will still apply to the correct points at shorter path lengths. Let I_m be mxm identity matrix and define,

$$\hat{I}_j = \left[\begin{array}{c|ccc} & I_b & 0 & 0 \\ I_{N_j} & 0 & 0 & 0 \\ & 0 & 0 & I_c \\ \hline 0 & & 0 & \end{array}\right], \quad (7)$$

where the 0 matrices are selected of the appropriate size.

Now, consider a process matrix constructed as in (6) for a path length N_1 as A_{N1} and another for a path length $N_2 > N_1$ as A_{N2}. Let x_1 and y_1 be the process input and output, respectively for A_{N1} such that, $y_1 = A_{N1} x_1$. It can be shown that,

$$\begin{bmatrix} y_1 \\ 0 \end{bmatrix} = \hat{I}_1 A_{N2} \begin{bmatrix} x_1 \\ x_2 \end{bmatrix}, \tag{8}$$

and thus the $\hat{I}$ matrix serves the purpose of recasting the process dynamics onto a shorter length path. For simplicity in later derivations, consider that A and B are constructed for the longest path length in the build and let,

$$A_j = \hat{I}_j A, \tag{9}$$

$$B_j = \hat{I}_j B, \tag{10}$$

where N_j is the length of the path on layer j.

In addition to the issues with periodically convolved geometry, the error matrix e_j must be resampled to match the length of the e_{j+1}. This may be accomplished by linearly interpolating between the closest two points at the previous layer as shown by Figure 7. The blue circle markers indicate the locations of points on the previous layer where the black asterisk markers represent the interpolated point locations both on the previous layer (blue lines) and as they are projected onto the following layer.

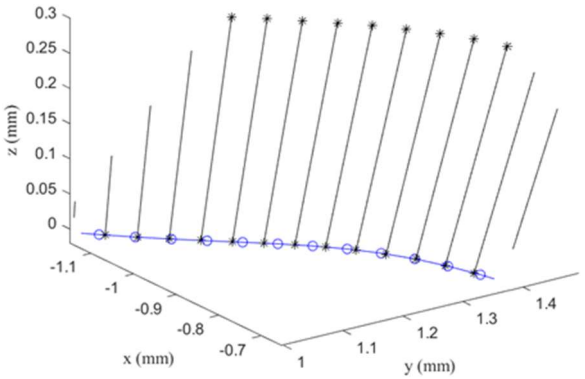

Figure 7: Interpolation of Points to Successive Layers

The $N_{max} \times N_{max}$ matrix T serves to resample the points and linearly interpolates between the closest two points on the previous iteration. An example of the interpolating nature of this matrix operator may be given as

$$T_j^{j+1} = \begin{bmatrix} t_{1,2} & 0 & 0 & \cdots & 0 & t_{1,1} & 0 & \cdots & 0 \\ t_{2,1} & t_{2,2} & 0 & & 0 & 0 & 0 & & 0 \\ t_{3,1} & t_{3,2} & 0 & & & & & & \\ 0 & t_{4,1} & t_{4,2} & & & & & & \vdots \\ 0 & t_{5,1} & t_{5,2} & & & & & & \\ \vdots & & & \ddots & & & & & \\ 0 & 0 & 0 & & t_{N_j-1,1} & t_{N_j-1,2} & 0 & & 0 \\ t_{N_j,2} & 0 & 0 & & 0 & t_{N_j,1} & 0 & & 0 \\ 0 & 0 & 0 & & 0 & 0 & 0 & & 0 \\ \vdots & & & & & & & \ddots & \vdots \\ 0 & 0 & 0 & \cdots & 0 & 0 & 0 & \cdots & 0 \end{bmatrix} \tag{11}$$

where $t_{i,1} + t_{i,2} = 1$ and both $t_{i,1}$ and $t_{i,2}$ are positive or zero (forcing interpolation instead of extrapolation). Implementing both $\hat{I}_j$ and T_j^{j+1}, the control structure takes the form,

$$e_{j+1} = A_{j+1} T_j^{j+1} e_j + B_{j+1} u_{j+1}. \tag{12}$$

IV. Repetitive Process Control Formulation

The RPC controller is designed using a similar quadratic-optimal approach as in [16]. Consider the cost function,

$$J = e_{j+1}^{\mathrm{T}} Q e_{j+1} + (u_{j+1} - u_j)^{\mathrm{T}} R (u_{j+1} - u_j) + u_{j+1}^{\mathrm{T}} S u_{j+1}. \tag{13}$$

Firstly, take the iteration prior to (12) as,

$$e_j = A_j T_{j-1}^{j} e_{j-1} + B_j u_j, \tag{14}$$

such that,

$$e_{j+1} - e_j = A_{j+1} T_j^{j+1} e_j + B_{j+1} u_{j+1} - A_j T_{j-1}^{j} e_{j-1} - B_j u_j. \tag{15}$$

Solving (15) for e_{j+1} and substituting the relationship into (13),

$$\begin{aligned} J = &\left(e_j + A_{j+1} T_j^{j+1} e_j - A_j T_{j-1}^{j} e_{j-1} + B_{j+1} u_{j+1} - B_j u_j \right)^{\mathrm{T}} Q \\ &\cdot \left(e_j + A_{j+1} T_j^{j+1} e_j - A_j T_{j-1}^{j} e_{j-1} + B_{j+1} u_{j+1} - B_j u_j \right) \\ &+ u_{j+1}^{\mathrm{T}} S u_{j+1} + \left(u_{j+1} - u_j \right)^{\mathrm{T}} R \left(u_{j+1} - u_j \right), \end{aligned} \tag{16}$$

where $Q=qI$, $R=rI$, and $S=sI$ are positive weighting matrices. While q, r, and s can be tuned to exact specific behaviors from the control structures (i.e. slower or faster learning, filtering structures), they were left as constants derived as in [21]. It can be shown that the cost function minimizes to,

$$\begin{aligned} 0 &= \frac{\partial J}{\partial u_{j+1}} \\ &= (B_{j+1}^{\mathrm{T}} Q B_{j+1} + S + R) u_{j+1} + B_{j+1}^{\mathrm{T}} Q e_j - \ldots \\ &\quad (B_{j+1}^{\mathrm{T}} Q B_j + R) u_j + B_{j+1}^{\mathrm{T}} Q (A_{j+1} T_j^{j+1} e_j - A_j T_{j-1}^{j} e_{j-1}). \end{aligned} \tag{17}$$

and solving (17) for u_{j+1} results in the relationship

$$u_{j+1} = L_e e_j + L_u u_j + L_{de} (A_{j+1} T_j^{j+1} e_j - A_j T_{j-1}^{j} e_{j-1}) \tag{18}$$

where,

$$L_u = (B_{j+1}^{\mathrm{T}} Q B_{j+1} + S + R)^{-1} (B_{j+1}^{\mathrm{T}} Q B_j + R) \tag{19}$$

$$L_e = L_{de} = -(B_{j+1}^{\mathrm{T}} Q B_{j+1} + S + R)^{-1} B_{j+1}^{\mathrm{T}} Q. \tag{20}$$

V. Experimental Results

A DED, blown powder AM machine shown in Figure 8 was used to implement the control formulation presented in (18). The machine consists of four nozzles which direct streams of metal powder (316L stainless steel with powder size 53-150μm in this case) into the path of a 1kW laser. The motion axes move the entire trunnion assembly in the horizontal directions while the deposition head moves vertically. The Keyence scanner was used between layers to

obtain height data on previous depositions. While the machine also has two rotary axes and is capable of 5-axis printing, only the translational axes were used in the experimental trials presented here.

Figure 8: LENS© Five-Axis Blown Powder Machine Workspace

The framework presented was implemented into a cone build with a 10-degree slope ($\alpha = 10°$) as shown in Figure 10 and Figure 12. Both specimens were built to a height of 26 mm (118 successive layers of deposition) using completely identical parameters varying only the control structure. The open-loop build (no control implemented) immediately developed instabilities which can be seen in the plot of the height at each layer in Figure 9. These initial instabilities propagated and intensified as the build progressed. While certain locations of the build did achieve the full height of the build, the overall quality of the build was entirely unacceptable for any reasonable application. Note that results after 50 layers were neglected in Figure 9 and Figure 11 for clarity and simplicity as general trends continued in both cases without much further development the majority of the later layers.

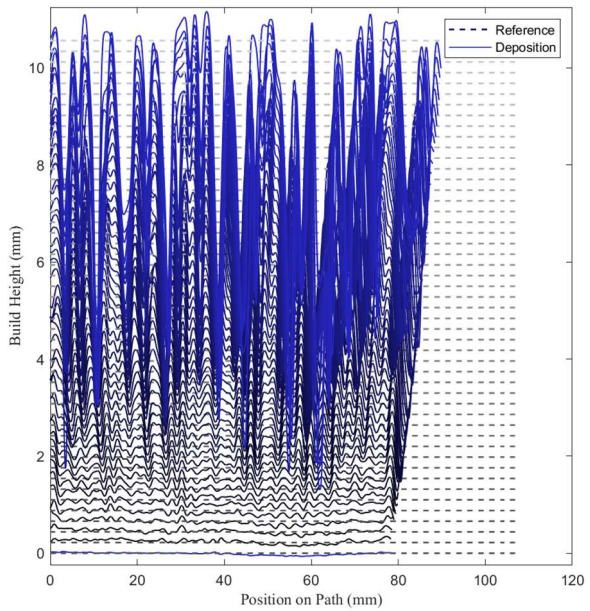

Figure 9: Layer Heights of Open-Loop 10-Degreee Cone Build

Figure 10: Open-Loop Trial of 10-Degreee Cone Build

The closed-loop trial implemented the above structure on the same build and successfully mitigated any disturbances present. The build showed some initial ripple instability which is apparent in most of the initial layers shown in Figure 11. These disturbances were learned by the controller and eliminated long before the completion of the build. While some variation is present in the thickness of the walls (a consequence of the application of the control), the layer height precision was more than satisfactory. Some slight variation may be observed at the start/end location (p_0), resulting from transient dynamics at initiation and termination of deposition, but have minimal impact.

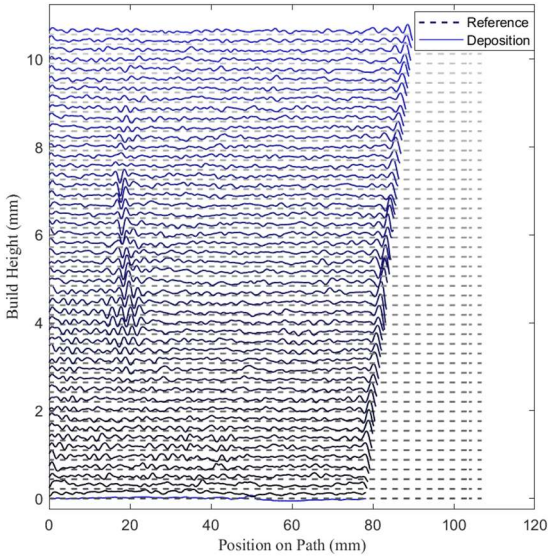

Figure 11: Layer Heights of Closed-Loop 10-Degreee Cone Build

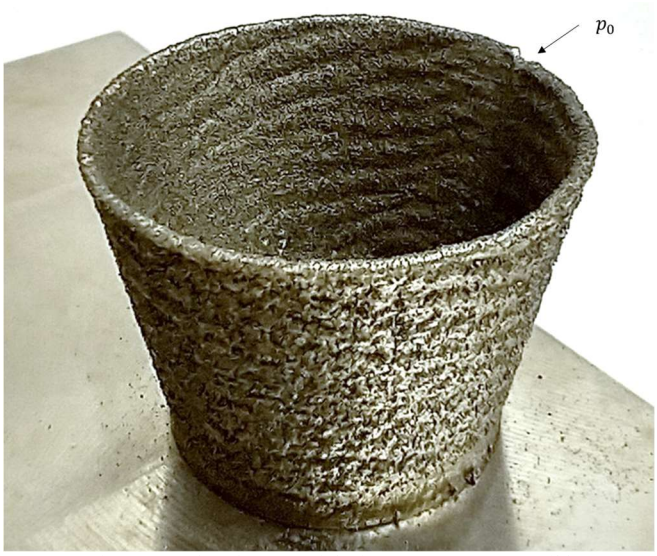

Figure 12: Closed-Loop Trial of 10-Degreee Cone Build

VI. Conclusion and Future Work

Single-wall builds are challenging for DED systems to accurately produce but are made even more difficult when the successive layers are not completely aligned with the deposition (as is the case in changing machine paths at successive layers). By applying and developing an interpolation method to the control structures developed in [16], more generalized build geometries may be constructed with reasonable accuracy.

The geometry of the build presented is simple when compared to the ideal scope of the presented control application. While physical limitations do exist, many more complex geometries and use-cases can be explored. Non-concentric and non-uniform expansions (provided they do not exceed process limitations) should also be achievable with the provided structure. These applications could assist with reducing waste and turnaround time in builds by eliminating infill where parts may be replaced with single wall builds. Notably, in applications where mass and density are crucial, single-walled structures could have enormous benefits. DED processes such as the blown powder method presented also have distinct advantages over traditional manufacturing methods and even SLM in terms of build complexity and orientation, which can be more fully utilized if build quality is improved with these RPC techniques.

Acknowledgment

The authors thank Dr. Michelle M. Gegel for support in the experimental implementation.

References

[1] B. Altın, Z. Wang, D. J. Hoelzle and K. Barton, "Robust Monotonically Convergent Spatial Iterative Learning Control: Interval Systems Analysis via Discrete Fourier Transform," *IEEE Transactions on Control Systems Technology,* vol. 27, no. 6, pp. 2470-2483.

[2] L. Tang and R. G. Landers, "Layer-to-Layer Height Control for Laser Metal Deposition Process," *ASME. J. Manuf. Sci. Eng. ,* vol. 133(2), p. art. num. 021009, 2011.

[3] L. Tang and R. Landers, "Melt Pool Temperature Control for Laser Metal Deposition Processes—Part II: Layer-to-Layer Temperature Layer-to-Layer Temperature," *Journal of Manufacturing Science and Engineering,* vol. 132(1), p. 011011, 2010.

[4] L. Tang, J. Ruan, T. E. Sparks, R. G. Landers and F. Liou, "Layer-to-layer height control of Laser Metal Deposition processes," in *2009 American Control Conference*, St. Louis, MO, USA , 2009.

[5] Z. Afkhami, D. Hoelzle and K. Barton, "Higher-Order Spatial Iterative Learning Control for Additive Manufacturing," in *60th IEEE Conference on Decision and Control (CDC)*, Austin, TX, USA, 2021.

[6] Z. Afkhami, D. Hoelzle and K. Barton, "Synthesis of model predictive control and iterative learning control for topography regulation in additive manufacturing," *IFAC-PapersOnLine,* vol. 55, no. 12, pp. 500-507, 2022.

[7] L. Aarnoudse, C. Pannier, Z. Afkhami, T. Oomen and K. Barton, "Multi-Layer Spatial Iterative Learning Control for Micro-Additive Manufacturing," *IFAC-PapersOnLine,* vol. 52, no. 15, pp. 97-102, 2019.

[8] M. J. B. Spector, Y. Guo, S. Roy, M. O. Bloomfield, A. Maniatty and S. Mishra, "Passivity-based Iterative Learning Control Design for Selective Laser Melting," in *2018 Annual American Control Conference* , Milwaukee, WI, USA, 2018.

[9] U. Inyang-Udoh, R. Hu, S. Mishra, J. Wen and A. Maniatty, "Model-free Multi-Objective Iterative Learning Control for Selective Laser Melting," in *2022 American Control Conference (ACC)*, Atlanta, GA, USA, 2022.

[10] A. Shkoruta, W. Caynoski, S. Mishra and S. Rock, "Iterative learning control for power profile shaping in selective laser melting," in *2019 IEEE 15th International Conference on Automation Science and Engineering (CASE)*, Vancouver, BC, Canada, 2019.

[11] P. M. Sammons, D. A. Bristow and R. G. Landers, "Control-Oriented Modeling of Laser Metal Deposition as a Repetitive Process," in *American Control Conference (ACC)*, Portland, Oregon, USA, 2014.

[12] P. M. Sammons, D. A. Bristow and R. G. Landers, "Two-Dimensional Modeling and System Identification of the Laser Metal Deposition Process," *Journal of Dynamic Systems, Measurement, and Control,* vol. 141 (2), p. art. no. 0210121, 2019.

[13] P. Sammons, D. Bristow and R. Landers, "Repetitive Process Control of Laser Metal Deposition," in *ASME 2014 Dynamic Systems and Control Conference*, San Antonio, Texas, USA, 2014.

[14] P. Sammons, D. Bristow and R. Landers, "A Model Predictive Repetitive Process Control Formulation for Additive Manufacturing Processes," in *Dynamic Systems and Control Conference*, Columbus, Ohio, USA, 2015.

[15] P. M. Sammons, M. L. Gegel, D. A. Bristow and R. G. Landers, "Repetitive Process Control of Additive Manufacturing With Application to Laser Metal Deposition," *IEEE Transactions on Control Systems Technology,* vol. 27, no. 2, pp. 566-575, 2019.

[16] D. M. Gegel, D. D. Bristow and D. R. Landers, "Quadratic Optimal Repetitive Process Control for Laser Metal Deposition," 2022.

[17] M. L. Gegel, D. A. Bristow and R. G. Landers, "A Loop-Shaping Method for Frequency-Based Design of Layer-to-Layer Control for Laser Metal Deposition," in *2020 American Control Conference (ACC)*, Denver, CO, USA, Denver, CO, USA.

[18] M. L. Gegel-Wainwright, "Layer-to-Layer Feedback Control For Direct Energy Deposition," Missouri University of Science and Technology, Rolla, Missouri, USA, 2021.

[19] M. Gegel, "DED Model Derivation," Missouri University of Science and Technology, Rolla, MO, 2022 (Unpublished).

[20] M. L. Gegel, D. A. Bristow and R. G. Landers, "Model Predictive Height Control for Direct Energy Deposition," in *Dynamic System and Control Conference*, Park City, Utah, 2019.

[21] M. L. Gegel, D. A. Bristow and R. G. Landers, "Layer-to-Layer Feedback Control for Direct Energy Deposition," Missouri University of Science and Technology, Rolla, Missouri, 2021 (Unpublished).